498

Egypt. J. Chem. **Vol. 65,** No. 8, pp. 65 - 75 (2022)

Egyptian Journal of Chemistry

http://ejchem.journals.ekb.eg/

Facile Synthesis and Characterization of Magnetic Biopolymer Nanocomposite and Its Application for Preparing Novel Bioasphalt Coating Binder

Hanan A. Ahmed[1],*, R.A. Geioushy[2], S. A. Elbanna[3], Ragab A. A. [4], Ibrahim M. Nassar[4], Hend Al‑aidy El‑saied[1]

[1] *Petrochemicals Department, Egyptian Petroleum Research Institute, Nasr City, Cairo 11727, Egypt*

[2] *Nanomaterials and Nanotechnology Department, Advanced Materials Division, Central Metallurgical R & D Institute (CMRDI), P.O. Box, 87 Helwan, 11421 Cairo, Egypt*

[3] *Processes Development Department, Egyptian Petroleum Research Institute, Nasr City, Cairo 11727, Egypt*

[4] *Petroleum Applications Department, Egyptian Petroleum Research Institute, Nasr City, Cairo 11727, Egypt*

Abstract

Magnetic bio-composites attract the attention of many researchers due to their unique properties. Also, using asphalt in industrial applications became very important according to environmental and economical issues. In this research, the chemical co-precipitation method was used to synthesize a magnetic biopolymer nanocomposite $CaNiFe_2O_4$@Chitosan with the weight ratios of 35 wt%/65 wt%. The synthesized nanocomposite was characterized by powder XRD, FTIR, VSM, S_{BET} and TEM techniques. Additionally, the nanocomposite was used for the preparation of a novel bio-asphalt coating binder. $CaNiFe_2O_4$@Chitosan was added to asphalt 60/70 with the percentages of 2, 4, 6, 8 and 10 % (wt/wt) to obtain a material with distinctive characteristics; novel nano-composite modified asphalt (NCMA). Also, it was tested to be applied in painting using the Konig pendulum. Additionally, the adhesion and dry-to-touch times were determined. This study reveals that the physical, mechanical, and rheological properties of asphalt binders can be improved to be used in different applications such as painting and coating by utilizing the synthesized $CaNiFe_2O_4$@Chitosan nanocomposite as a biomodifier.

Keywords: Magnetic biopolymer; Nanocomposite; Synthesis; Characterization; Bioasphalt coating binder

1. Introduction

In earlier periods, various asphalts were used in coatings in the pipeline industry for a wide range of applications to reduce the destructive effects of chemicals and weather [1, 2]. Due to its inherent cohesive nature, low cost, waterproofing, anti-corrosion properties, and rheological behavior, asphalt is still used as a coating [3]. Soft asphalt exhibits poor chemical, thermal and physico-mechanical properties. Soft asphalt materials also have low cohesion strength at ambient temperature. And with cooling, the painted surfaces are exposed to cracks as a result of which become fragile and weak and may be exposed to damage with transportation and use. Therefore, improving the physical, mechanical, and chemical properties of asphalt to develop high-quality, safe, reliable, and environmentally-friendly modified asphalt materials became an urgent necessity by adding modifiers [4, 5]. Various additives including polymers, nanocomposites, fillers, and others, are used to improve the asphalt binder properties. Among the mentioned additives, the best results were obtained for polymers as modifiers to enhance the rheological and mechanical characteristics of asphalt binders [6-8]. Between all polymer modifiers, SBR (Styrene butadiene rubber) is one of the most commonly used polymers for modifying asphalt [9]. Its addition to

bitumen improves properties like low-temperature ductility and elastic recovery in asphalt. Also, SBR polymers addition increases the flexibility and ductility of asphalt binder, which enhances crack resistance at low temperatures [10]. However, the use of pure polymer as an asphalt binder modifier has a high cost and to reduce the polymeric modifier cost, several works have been aimed to evaluate the use of biomodifiers in asphalt binders. The previous research works demonstrated that the use of biomodifiers is a promising area that requires further study [11]. Therefore, the development of eco-friendly asphalt binders based on biopolymers is very important to produce green coatings. Chitosan is a biopolymer composed of D-glucosamine and N-acetyl-D-glucosamine units [12]. Its properties are mainly governed by the acid-base properties of the amine group. It has been employed for different green applications such as coatings, adsorption of pollutants from wastewater, and corrosion inhibitors due to its rich surface functional group, low price, and renewable advantages [13-15]. The presence of primary amine ($-NH_2$) and hydroxyl ($-OH$) reactive groups in the chemical structure of chitosan may be used for its chemical functionalization [16, 17]. The chemical modification of chitosan with new grafts and converting their molecular sizes from macro to nanocomposites were carried out to improve their metal protection applications [18, 19]. Fabrication of nanocomposite polymers donates unique mechanical properties in comparison to pure polymers or micro and macro composites [20-22]. Behnam Amini approved that the existence of nanoclay (NC) in SBR improves storage stability, and increases the indirect strength of asphalt mixture [23]. Zhang Baochang also used SBR/montmorillonite (MMT) nanocomposite for improving the viscoelastic properties of asphalt binder and its high resistance to rutting [24]. Additionally, applying magnetic nanoparticles is increasing in fundamental and applied researches due to their fascinating properties such as non-toxicity, high efficiency, and the plausibility of synthesizing them in the laboratory from various iron precursors at relatively low-cost [25, 26]. Different types of Fe_2O_3-grafted polymer nanocomposites have been synthesized, such as Fe_2O_3 based on poly(methyl methacrylate), Fe_2O_3-grafted polypropylene and Fe_2O_3 based on polystyrene, and so on [27-29]. The obtained products show an improving in the rheological and the physical properties of the resultant composites and solving the problem of sedimentation of Fe_2O_3 particles in industrial applications. Within this context, the co-precipitation method was used to synthesize a magnetic biopolymer nanocomposite $CaNiFe_2O_4$@Chitosan with the weight ratios of 35 wt%/65 wt%. The synthesized nanocomposite structural, magnetic, and morphological

characteristics were examined by XRD, FTIR, S_{BET}, VSM, and TEM techniques. Additionally, it was studied as a biomodifier in asphalt application for the first time. It was added to asphalt 60/70 with the percentages of 2, 4, 6, 8, and 10 % (wt/wt) to obtain a material with distinctive characteristics; novel bio-asphalt coating binder. Also, it was tested to be applied in painting using the Konig pendulum (TS6041/EN ISO 1522). Lastly, we determined the adhesion by a cross-cut test (TS4313/EN ISO 2409) and the dry to touch times according to ASTM 1640.

2. Materials and Methods

2.1. Materials

Nickel nitrate [Ni $(NO_3)_2$ .6H_2O], ferric nitrate [Fe $(NO_3)_3$ .9H_2O], and calcium chloride ($CaCl_2$) were purchased from Sigma–Aldrich. Chitosan (Mw =150$\times$ 10^3 Da, deacetylation degree 82.5%) was obtained from Fluka. Acetic acid (CH_3COOH) was obtained from Merck Chemical Co. All chemicals were not purified before utilization.

2.2. Synthesis of CaNiFe$_2$O$_4$@Chitosan magnetic nanocomposite

A magnetic biopolymer nanocomposite $CaNiFe_2O_4$@Chitosan with the weight ratios of (35 wt%/65 wt%) was synthesized by the chemical co-precipitation method. Typically, clear solutions of metal precursors ($CaCl_2$, Ni $(NO_3)_2$. 6H_2O, and Fe $(NO_3)_3$. 9H_2O) with the weight ratios of 5 wt%: 10 wt%: 20 wt%, respectively; were prepared by their separate dissolution in three beakers each containing 30 mL of distilled water. The obtained solutions were mixed under stirring at 450 rpm for 60 min until a homogenous solution was obtained. Under stirring at 650 rpm, a simultaneous dropwise addition of NaOH solution (5 mol/L) and chitosan solution (65 wt% of chitosan was dissolved previously in acetic acid solution (1 mol/L) to the abovementioned ferrite solution was occurred. The stirring was maintained at 65 °C for a further 2 h till the formation of ferrite beads. The obtained particles were then collected using an external magnet and washed repeatedly with de-ionized water. Then, dried at 100 °C for 12 h and saved for further use and analysis.

2.3. Preparation of nanocomposite modified asphalt (NCMA)

All the asphalt-nanocomposite blends were prepared in an appropriate container equipped with a high shear mixer (HSM-1001C, Ross). A known quantity of the asphalt binder was added to the container and heated to 160 °C, followed by the addition of the nanocomposite in the hot asphalt over 5 min at 1500

rpm. The mixture was continuously stirred for further 15 min under the same conditions and then for another 45 min at 5000 rpm at a temperature-controlled between 180 and 190 °C. The runs were conducted with 2, 4, 6, 8 and 10 % (w/w) of the synthesized nanocomposite to prepare the nanocomposite modified asphalt (NCMA) samples [30]. The prepared samples were named as NCMA 2%, NCMA 4%, NCMA 6%, NCMA 8% and NCMA 10%.

2.4. Characterization of the synthesized $CaNiFe_2O_4$@Chitosan nano-composite

Fourier Transform Infrared (FTIR) spectroscopic measurement over the wavenumber 4000-400 cm^{-1}, using KBr pellets was recorded on the Nicolet IS-10 FTIR model. The crystalline phase of the sample was analyzed using powder X-ray diffraction performed at room temperature using X'Pert PRO PANalytical diffractometer with Cu Ka radiation at a scanning rate of 0.05 S^{-1} in the 2θ range of 6-66°. The surface area study was performed by N$_2$- adsorption desorption isotherm at 77 K using Nova- Touch LX4, Quantachrome, USA. Barrett, Joyner, and Halenda (BJH) equation was used to measure the adsorption results [31]. The magnetic properties were evaluated using a vibrating sample magnetometer (VSM 7407, Lake Shore, USA) at a temperature of 25 ℃. The morphology of the nano-composite was studied by TEM (JEM-200CX, JEOL 2100, Japan) at an accelerating voltage of 200 kV.

2.5. Characterization of the prepared nanocomposite modified asphalt (NCMA)

2.5.1. Rheological characterization

The rheological behavior of the virgin asphalt binder and the prepared nano-composite modified asphalt (NCMA) mixtures were analyzed in a dynamic shear rheometer (Anton Paar RheoCompass™ smart pave 102, V1.20.496-Release) following a test procedure and sample preparation method. The tests were undertaken under controlled-strain loading conditions using different test temperatures as 58, 64, 70, and 76 °C, with a 25 mm diameter, 1 mm gap parallel plate testing geometry, frequency of 10 rad/s, and strain of 12%. The strain amplitude was confined within the linear viscoelastic response of the asphalt binder [32].

2.5.2. Paint tests

The paints were applied on carbon steel panels, the physical properties were determined after 2 weeks. Hardness was determined by the Konig pendulum (TS6041/EN ISO 1522). Adhesion was determined by a cross-cut test (TS4313/EN ISO 2409). Dry-to-

touch times were determined according to ASTM 1640. The test panels were coated after brushed and prepared with the materials to be tested and allowed to dry for 3 days. The edges were coated dipping in molten paraffin wax. The coated panels were immersed in an aqueous solution containing 5 g of sodium hydroxides, sulphuric acid (sp. gr. 1.84) per 100 mL of water both alone and tap water for 4 h or any specified time intervals. The panels were removed, washed and the film examined immediately after drying for 1 h for any defect.

2.5.3. Mandrel bending test (ASTM D 522, 2013)

Mandrel test is used to evaluate the flexibility of coated strip metal that is to be formed during a fabrication process. ASTM D522 contains two test methods that are used to determine the flexibility and resistance to cracking of organic coatings on substrates of sheet metal. The coating material was applied at a uniform thickness to panels of sheet metal. After full curing, the coated panels were bent over a mandrel and the resistance to cracking of the coating was determined. Coatings attached to substrates are elongated when the substrates are bent during the manufacture of articles or when the articles are abused in service. Conical mandrel bend tester is applicable to determine the extensibility of coatings on metal panels that are clamped in position and formed round the conical mandrel by rotating the roller frame. The panels are examined to evaluate crack resistance detachment from the metal substrate of the coated surface which is coated with epoxy under standard conditions. In this study, the samples were kept at a very low temperature in the refrigerator (less than 23 ℃) as severe conditions.

2.5.4. Drying time (D 1640, 2003)

This test method describes the determination of several stages and the rate of dry-film formation of the prepared bio-asphalt coatings using straight lines and circular mechanical drying-time recording devices. This test is carried out by a simple technique. The time at which a metal panel is coated with the coating material and left to dry in a horizontal position at the ordinary condition of temperature and relative humidity is known as drying time.

3. Results and Discussion

3.1. FTIR spectra

The FTIR spectrum of $CaNiFe_2O_4$@Chitosan nanocomposite is displayed in Fig. 1. The three-strong bands located at 880 cm^{-1}, 950 cm^{-1}, and 1016 cm^{-1} are due to the saccharide structure of chitosan [33-35]. The absorption bands recorded at 1437 cm^{-1}, and at 1579 cm^{-1} and 1626 cm^{-1} are, respectively, correlated to the symmetrical deformation mode or rocking of the CH$_3$ group and the stretching

vibrations of the amide groups [35-37]. The broad band centered at 3425 cm^{-1} is due to the overlapped symmetric stretching vibration of the O–H and N-H groups [38]; while the sharp band centered at 3646 cm^{-1} is due to the -NH$_2$ groups of chitosan. Additionally, the stretching vibrations of the aliphatic –CH$_2$ and –CH$_3$ groups are, respectively, recorded at 2920 and 2839 cm^{-1} [39]. Besides the two specific bands observed in the range of 700-350 cm^{-1}, are assigned to M-O (M–metallic cation, O-oxygen anion) stretching vibration, while the third band appeared at 778 cm^{-1} is due to the cation exchange between the octahedral and tetrahedral sites [39, 40]. Finally, the sharp band that appeared at 880 cm^{-1} is assigned to a unique vibration for calcium oxide (Ca-O) [41]. The existence of chitosan main bands with some other bands attached to the CaNiFe$_2$O$_4$ nanoparticles revealed the successful synthesis of CaNiFe$_2$O$_4$@Chitosan nanocomposite.

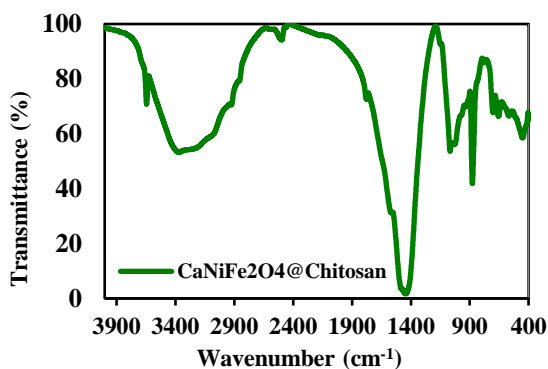**Fig. 1:** FTIR spectrum of CaNiFe$_2$O$_4$@Chitosan nanocomposite

3.2. XRD analysis

The X-ray diffraction patterns of CaNiFe$_2$O$_4$@Chitosan nanocomposite are depicted in Fig. 2. The nanocomposite XRD patterns proved its crystalline structure. The characteristic peaks of chitosan are observed at 2θ of 16°, 28°, 34° and 41° [16, 42]. While, the most two characteristic reflections of spinel structure formation are observed at 2θ of 29° and 35º [39, 43]. The mentioned results confirmed the successful synthesis of CaNiFe$_2$O$_4$@Chitosan nanocomposite.

3.3. Texture properties

N$_2$ adsorption-desorption isotherm of the synthesized CaNiFe$_2$O$_4$@Chitosan nanocomposite was shown in Fig. 3. The isotherm can be classified as type-IV according to IUPAC classification exhibiting H3 hysteresis loop at a relative pressure range of about

0.6–1.0, revealing the presence of mesoporous structure with slit-like shaped pores [44]. Additionally, the specific surface area results listed in Table 1 indicate that the total pore volume, pore diameter, and the BET surface area of the nanocomposite are 0.20 cc/g, 2.61 nm, and 71.65 m^2/g, respectively.

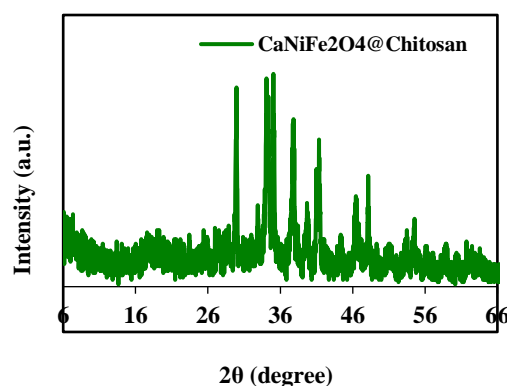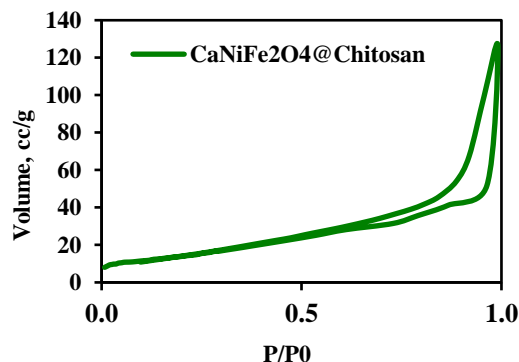**Fig. 2:** XRD of CaNiFe$_2$O$_4$@Chitosan nanocomposite

Fig. 3: N$_2$ adsorption-desorption isotherm of CaNiFe$_2$O$_4$@Chitosan nanocomposite

Table 1 Surface characteristics of the synthesized CaNiFe$_2$O$_4$@Chitosan nanocomposite

Sample	S$_{BET}$, m^2/g	Pore volume, cc/g	Pore diameter, nm
CaNiFe$_2$O$_4$@Chitosan	71.650	0.202	2.611

3.4. VSM analysis

The magnetic properties of the synthesized CaNiFe$_2$O$_4$@Chitosan nanocomposite were studied by VSM analysis. The VSM results are represented in the magnetization curve (Fig. 4). The saturation

magnetization of CaNiFe$_2$O$_4$@Chitosan was 37.58emu/g confirming that the synthesized nanocomposite has a superparamagnetic behavior [45].
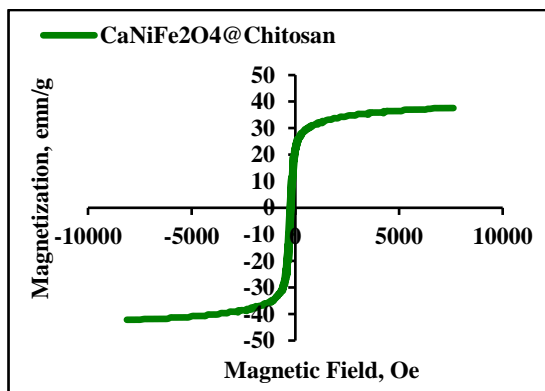

Fig. 4: VSM analysis of CaNiFe$_2$O$_4$@Chitosan nanocomposite

3.5. TEM

Figure 5 showed the TEM photograph of the synthesized CaNiFe$_2$O$_4$@Chitosan nanocomposite. The TEM image reveals that the CaNiFe$_2$O$_4$ NPs are incorporated into the porous structure of chitosan and the resulting composite is in the nanoscale.

3.6. Physical properties of the modified asphalt samples

Results in Table 2 illustrate that the addition of the prepared nano-composite modified asphalt (NCMA) as a biomodifier to virgin asphalt (Ac) caused an increase in its stiffness which can be easily shown as the penetration values decreased as the additional content increased up to 10% in a percent of 66.6%. For example, the penetration value decreased from 63 to 34 by the addition of 6% NCMA. The softening point temperature increased as the additional content increased. The value increased from 46 to 76 °C in a percent of 65.2% for 8% NCMA addition. The penetration index increased as the additional content increased. For example, the (PI) value increased from - 1.742 to 2.117 by the addition of 8% NCMA resulting in a biomodifier with lower temperature susceptibility and more resistance to cracking at low temperatures. Also, the dynamic viscosity at 135 °C increased obviously from 912 to 1310 mPa.s. in a percent of 43.6% due to the addition of 4% NCMA.
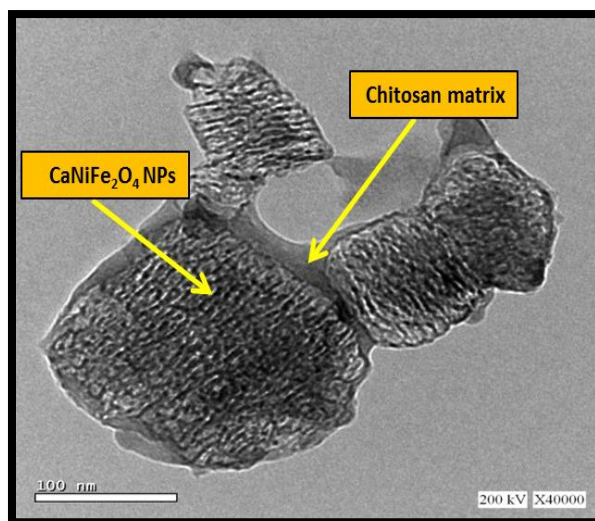

Fig. 5: TEM images of CaNiFe$_2$O$_4$@Chitosan nanocomposite

Table 2: Physical properties of virgin asphalt and modified asphalt samples

Characteristics	Virgin Asphalt (Ac)	NCMA 2%	NCMA 4%	NCMA 6%	NCMA 8%	NCMA 10%
Penetration at 25 °C, 0.1 mm	63	49	41	34	25	21
Softening Point (Ring &Ball), °C	46	62	67	71	76	80
Penetration index (PI)	- 1.742	1.365	1.829	2.043	2.117	2.309
Specific Gravity at 25 °C	1.019	1.038	1.051	1.075	1.089	1.131
Ductility at 25 °C, cm	+100	+100	+100	+100	+100	90.0
Dynamic Viscosity at 135 mPa.s	912	1281	1310	1370	1410	1438

3.7. Rheological properties

3.7.1. Complex shear modulus

The complex shear modulus master of the modified asphalt binder and control asphalt binder are displayed in Fig. 6. It can be described that the complex modulus (G*) values of modified asphalt binders are less than the control asphalt binder, and the complex shear modulus (G*) values of 4% NCMA binder are close to that of control asphalt binder at low temperatures. With the addition of 4% NCMA in the control asphalt binder, the complex shear modulus decreased by an average of 33.9% while the 2% NCMA addition just decreased by an average of 58.3%. From Fig. 6, the complex shear modulus of NCMA binder is decreased relative to the control asphalt. That means that the addition of NCMA in the control asphalt improves the resistance to rutting. Therefore, NCMA binder may have better performance of resistance to rutting relative to the control asphalt binder [46].
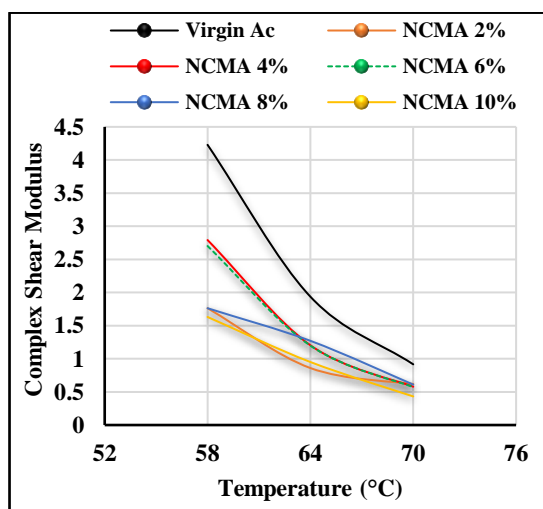

Fig. 6: complex shear modulus of virgin and modified samples at different temperatures

3.7.2. Phase angel (δ)

Figure 7 shows the phase angle of the virgin and the NCMA samples containing 2, 4, 6, 8, and 10% (wt/wt). From this figure, it is shown that the modified samples are all slightly higher than that of virgin binders. It means that these asphalts samples have less elastic recovery performance than their virgin asphalt. This indicates that the addition of the

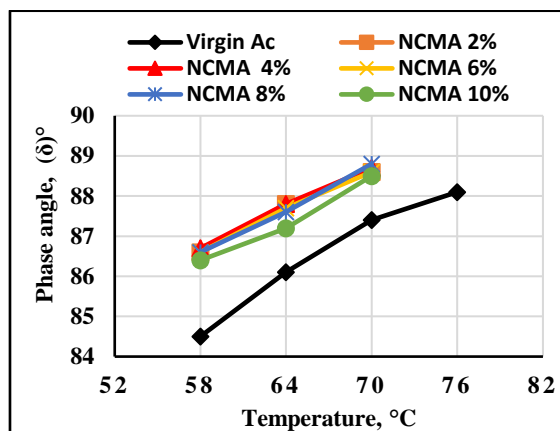modifying agent has less impact on the elastic recovery performance than that of virgin asphalt [47].

Fig. 7: The phase angle of the virgin and the modified asphalt samples at different temperatures

3.7.3. Rutting parameter (G*/ Sin δ)

Figure 8 shows the (G*/sin δ) versus temperature curves for the virgin and modified asphalt binders. The G*/sin δ values were calculated for the temperatures of 58, 64, 70, and 76 °C and increased during the aging process. The results show that the magnetic biopolymer addition to the asphalt decreases significantly the G*/sinδ value and this extends the temperature range within which it can be used. Although the modifying agent decreases the G*/sin δ values due to the plasticizer effect, these are still sufficiently high and the modified samples can be used within a wider temperature range in comparison to the pure asphalt binder. From observing the G*/sin δ values before and after adding the modifying agent it is possible to state that the modified asphalt can be used below 70 °C because the G*/sin δ values of these samples at 70 °C are higher than the values of 1.0 kPa obtained after adding the modifying aging [48].
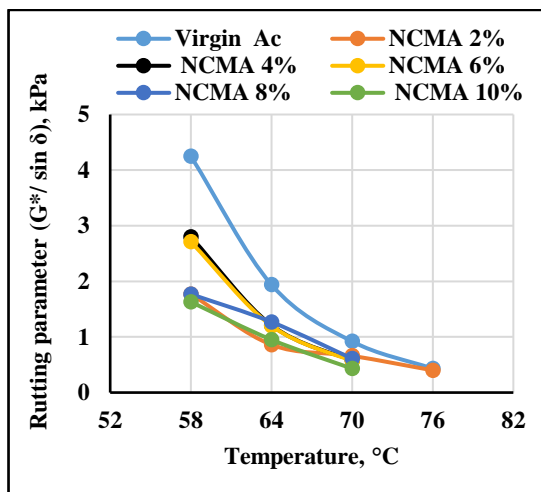
Fig. 8: Rutting parameter of virgin and modified samples at different temperatures

3.8. Chemical resistance

From the study of the resistance to external media at room temperature and relative humidity of about 50%, the obtained data are given in Table 3 show that the addition of the prepared nano-composite greatly improved the chemical resistance of the prepared oxidizing bitumen formulations, as compared with unmodified one. The modified sample has very good water resistance, dilute acid, dilute alkalis, aliphatic hydrocarbons resistance, furthermore having a good resistance when exposed to oils and greases, alcohols, but having poor resistance when exposed to aromatic-hydrocarbons [49].

3.9. Paint tests

The results of the above studies show that the modification of paints with the prepared NCMA has resulted in improvement in their properties i.e. adhesion, hardness and impact, by increasing the content of the added NCMA. Also, Table 4 shows that the dry hard time varied from 100 h to 38 h while the complete dry time for the different paints is varied from 140 h to 54 h which demonstrates that the modified paints with the prepared nano-composite are better than the non-modified paints. From these results, it can be inferred that the performance of the modified paints based on the prepared NCMA is superior to the unmodified paints [50].

Table 3: Resistance to different media for both the blank samples and those modified with NCMA, at room temperature

Medium	Water						5% H_2SO_4						5% NaOH					
Time/h	4	8	24	48	72	168	4	8	24	48	72	168	4	8	24	48	72	168
Unmodified	+	+	+	+	+	+	+	+	+	+	-	-	+	+	+	+	-	-
NCMA 2%	+	+	+	+	+	+	+	+	+	+	+	+	+	+	+	+	+	+
NCMA 4%	+	+	+	+	+	+	+	+	+	+	+	+	+	+	+	+	+	+
NCMA 6%	+	+	+	+	+	+	+	+	+	+	+	+	+	+	+	+	+	+
NCMA 8%	+	+	+	+	+	+	+	+	+	+	+	+	+	+	+	+	+	+

(-) nonresistance   (+) resistance   (NCMA) Nano-composite modified asphalt samples

Table 4: Properties of the prepared paints

Experiment	Virgin paints	NCMA 2%	NCMA 4%	NCMA 6%	NCMA 8%	NCMA 10%
Tacky (finger print) (h)	5	3	2	1.5	1.5	1.3
Dry Hard (h)	100	80	65	55	43	38
Complete dry (h)	140	100	80	67	59	54
Adhesion	poor	good	good	excellent	excellent	excellent
Hardness (s)	poor	good	good	excellent	excellent	excellent
Impact	good	good	good	excellent	excellent	excellent

_____

3.10. Mandrel bending test

Coatings attached to substrates are elongated when the substrates are bent during the manufacture of articles or when the articles are abused in service. So, this test method is useful in rating attached coatings for their ability to resist cracking when elongated i.e. measure the flexibility of coatings on flexible substrates. Based on ASTM D522 and from Fig. 9a-f we can find that Ac (freeze at 0 ºC) and oxidized asphalt (OA) samples when elongated with Mandrel bending tester the cracks appear on the panel. On the other hand, from the corresponding elongation to such added values of the polymer, it is clear that when the nano-composite content increased to 10%, the sample becomes completely flexible and no cracks appear as shown in Fig. 9a-f. Mandrel test clearly showed that incorporating 8% of NCMA enhances the flexibility of the modified asphalt samples to the required value as a result of the formation of a strong network between the added magnetic biopolymer and asphalt.

3.11. Drying time test

From Table 5 it is noticed that the drying time of virgin asphalt (Ac) is 72 h due to its high viscosity at room temperature which is unacceptable for industrial applications. For the oxidized asphalt (OA), because the oxidation process leads to the hardening of the material and increases the cracking probability, there is no time for drying i.e. the sample dried immediately. From this table, it is also found that the drying time is highly decreased in the case of using the prepared NCMA compared to the virgin asphalt sample. This is due to the nature of the added nanocomposite itself. From data, the drying time decreased by 55.5, 61.1, 66.6, 72.2%, and 61.1%. Finally, using the prepared nanocomposite decreased the drying time of the prepared bioasphalt binder samples and became suitable for use as coating materials.

Fig. 9: Mandrel bend testing panel of **a)** virgin asphalt (Ac), **b)** Oxidized asphalt, and bioasphalt binder containing **c)** 2% NCMA, **d)** 4% NCMA, **e)** 6% NCMA, and **f)** 8 % NCMA.

_____

Table 5: Curing time for the prepared bioasphalt binders

Sample Type	Curing Time (h)
Ac	72
OA	No time
2% NCMA	32
4% NCMA	28
6% NCMA	24
8% NCMA	20
10% NCMA	28

4. Conclusion

In this research, a promising magnetic biopolymer nanocomposite $CaNiFe_2O_4$@Chitosan with the weight ratios of 35 wt%/65 wt% was successfully synthesized as confirmed by various analytical techniques. Novel bio-asphalt coating binders were prepared by adding 2, 4, 6, 8 and 10 % (wt/wt) of $CaNiFe_2O_4$@Chitosan nano-composite to asphalt 60/70. Also, the synthesized magnetic biopolymer was examined to be applied in painting using the Konig pendulum test. The results of this study revealed that the physical, mechanical, and rheological properties of asphalt were improved by utilizing the synthesized $CaNiFe_2O_4$@Chitosan nanocomposite as a magnetic biomodifier. The obtained results also revealed that the nanocomposite addition improved the complex shear modulus, phase angle, and rutting resistance parameter of the modified samples. Additionally, its addition to asphalt was greatly improved the chemical resistance of the prepared oxidizing bitumen formulations as compared with unmodified ones. Moreover, the prepared bioasphalt binders can be used as promising coating materials and in the painting industry due to their excellent properties.

Conflict of Interest: The authors declare that they have no conflict of interest.

References

[1] S.D. Jagtap, S.P. Tambe, R.N. Choudhari, B.P. Mallik, Mechanical and anticorrosive properties of non toxic coal-tar epoxy alternative coating, Progress in Organic Coatings 77(2) (2014) 395-402.

[2] H. Shi, T. Xu, P. Zhou, R. Jiang, Combustion properties of saturates, aromatics, resins, and asphaltenes in asphalt binder, Construction and Building Materials 136 (2017) 515-523.

[3] Y. Xiao, M.F.C. van de Ven, A.A.A. Molenaar, S.P. Wu, Possibility of using epoxy modified bitumen to replace tar-containing binder for pavement antiskid surfaces, Construction and Building Materials 48 (2013) 59-66.

[4] O. González, J.J. Peña, M.E. Muñoz, A. Santamaría, A. Pérez-Lepe, F. Martínez-Boza, C. Gallegos, Rheological Techniques as a Tool To Analyze Polymer−Bitumen Interactions: Bitumen Modified with Polyethylene and Polyethylene-Based Blends, Energy Fuels 16(5) (2002) 1256-1263.

[5] R. Li, F. Xiao, S. Amirkhanian, Z. You, J. Huang, Developments of nano materials and technologies on asphalt materials – A review, Construction and Building Materials 143 (2017) 633-648.

[6] E.M. Abdel Bary, R.K. Farag, A.A. Ragab, R.M. Abdel-monem, Z.L. Abo-shanab, A.M.M. Saleh, Green asphalt construction with improved stability and dynamic mechanical properties, Polymer Bulletin 77(4) (2019) 1729-1747.

[7] S.G. Jahromi, A. Khodaii, Effects of nanoclay on rheological properties of bitumen binder, Construction and Building Materials 23(8) (2009) 2894-2904.

[8] G. Polacco, J. Stastna, D. Biondi, L. Zanzotto, Relation between polymer architecture and nonlinear viscoelastic behavior of modified asphalts, Current Opinion in Colloid & Interface Science 11(4) (2006) 230-245.

[9] A. Sakr, A. Naser, H. Abd El-Wahab, M. Abd El-Fattah, A. Mostafa, Preparation and characterization of modified reclaimed asphalt by using styrene – butyl acrylate nanoemulsion copolymer, Egyptian Journal of Chemistry 61(2) (2018) 280-290.

[10] M.G. Bouldin, J.H. Collins, Influence of Binder Rheology on Rut Resistance of Polymer Modified and Unmodified Hot Mix Asphalt, Polymer Modified Asphalt Binders, ASTM International, pp. 50-50-11.

[11] S. Caro, N. Vega, J. Husserl, A.E. Alvarez, Studying the impact of biomodifiers produced from agroindustrial wastes on asphalt binders, Construction and Building Materials 126 (2016) 369-380.

[12] R.-S. Juang, F.-C. Wu, R.-L. Tseng, Solute adsorption and enzyme immobilization on chitosan beads prepared from shrimp shell wastes, Bioresource Technology 80(3) (2001) 187-193.

[13] H. Ashassi-Sorkhabi, A. Kazempour, Chitosan, its derivatives and composites with superior potentials for the corrosion protection of steel alloys: A comprehensive review, Carbohydrate Polymers 237 (2020) 116110.

[14] A. Baggio, H.N. Doan, P.P. Vo, K. Kinashi, W. Sakai, N. Tsutsumi, Y. Fuse, M. Sangermano, Chitosan-Functionalized Recycled Polyethylene Terephthalate Nanofibrous Membrane for Sustainable On-Demand Oil-Water Separation, Glob Chall 5(4) (2021) 2000107-2000107.

[15] M.F. Mubarak, A.H. Ragab, R. Hosny, I.A. Ahmed, H.A. Ahmed, S.M. El-Bahy, A. El Shahawy, Enhanced Performance of Chitosan via a Novel Quaternary Magnetic Nanocomposite Chitosan/Grafted Halloysitenanotubes@ZnγFe(3)O(4) for Uptake of Cr (III), Fe (III), and Mn (II) from Wastewater, Polymers 13(16) (2021) 2714.

[16] H.A. Ahmed, M.F. Mubarak, Adsorption of Cationic Dye Using A newly Synthesized CaNiFe2O4/Chitosan Magnetic Nanocomposite: Kinetic and Isotherm Studies, J. Polym. Environ. 29(6) (2021) 1835-1851.

[17] P. Zhao, N. Qin, C.L. Ren, J.Z. Wen, Surface modification of polyamide meshes and nonwoven fabrics by plasma etching and a PDA/cellulose coating for oil/water separation, Applied Surface Science 481 (2019) 883-891.

[18] N. Illy, S. Benyahya, N. Durand, R. Auvergne, S. Caillol, G. David, B. Boutevin, The influence of formulation and processing parameters on the thermal properties of a chitosan-epoxy prepolymer system, Polymer International 63(3) (2013) 420-426.

[19] M. Shibata, J. Fujigasaki, M. Enjoji, A. Shibita, N. Teramoto, S. Ifuku, Amino acid-cured bio-based epoxy resins and their biocomposites with chitin- and chitosan-nanofibers, European Polymer Journal 98 (2018) 216-225.

[20] H.A. Ahmed, M.S.S. Soliman, S.A. Othman, Synthesis and Characterization of Magnetic Nickel Ferrite-Modified Montmorillonite Nanocomposite For Cu (II) and Zn (II) Ions Removal From Wastewater, Egyptian Journal of Chemistry 0(0) (2021) 0-0.

[21] H.M. Naguib, M.A. Ahmed, Z.L. Abo-Shanab, Silane coupling agent for enhanced epoxy-iron oxide nanocomposite, Journal of Materials Research and Technology 7(1) (2018) 21-28.

[22] H.M. Naguib, M.A. Ahmed, Z.L. Abo-Shanab, Studying the loading impact of silane grafted Fe2O3 nanoparticles on mechanical characteristics of epoxy matrix, Egyptian Journal of Petroleum 28(1) (2019) 27-34.

[23] B. Amini, M.J. Rajabbolookat, A. Abdi, R. Salehfard, Investigating the influence of using nano-composites on storage stability of modified bitumen and moisture damage of HMA, Petroleum Science and Technology 35(8) (2017) 800-805.

[24] B. Zhang, M. Xi, D. Zhang, H. Zhang, B. Zhang, The effect of styrene–butadiene– rubber/montmorillonite modification on the characteristics and properties of asphalt, Construction and Building Materials 23(10) (2009) 3112-3117.

[25] P. Xu, G.M. Zeng, D.L. Huang, C.L. Feng, S. Hu, M.H. Zhao, C. Lai, Z. Wei, C. Huang, G.X. Xie, Z.F. Liu, Use of iron oxide nanomaterials in wastewater treatment: A review, Sci. Total Environ. 424 (2012) 1-10.

[26] S. Yu, X. Wang, Y. Ai, X. Tan, T. Hayat, W. Hu, X. Wang, Experimental and theoretical studies on competitive adsorption of aromatic compounds on reduced graphene oxides, Journal of Materials Chemistry A 4(15) (2016) 5654-5662.

[27] Y.J. Kim, Y.D. Liu, Y. Seo, H.J. Choi, Pickering-Emulsion-Polymerized Polystyrene/Fe2O3 Composite Particles and Their Magnetoresponsive Characteristics, Langmuir 29(16) (2013) 4959-4965.

[28] A. Laachachi, E. Leroy, M. Cochez, M. Ferriol, J.M. Lopez Cuesta, Use of oxide nanoparticles and organoclays to improve thermal stability and fire retardancy of poly(methyl methacrylate), Polymer Degradation and Stability 89(2) (2005) 344-352.

[29] J. Zhu, Q. He, Z. Luo, A. Khasanov, Y. Li, L. Sun, Q. Wang, S. Wei, Z. Guo, Property manipulated polypropylene–iron nanocomposites with maleic anhydride polypropylene, J. Mater. Chem. 22(31) (2012) 15928.

[30] M.R.S. Fernandes, M.M.C. Forte, L.F.M. Leite, Rheological evaluation of polymer-modified asphalt binders, Materials Research 11(3) (2008) 381-386.

[31] F.H.H. Abdellatif, M.M. Abdellatif, Bio-based i-carrageenan aerogels as efficient adsorbents for heavy metal ions and acid dye from aqueous solution, Cellulose 27(1) (2019) 441-453.

[32] H. Soenen, X. Lu, P. Redelius, The morphology of SBS modified bitumen in binders and in asphalt mix, Advanced Testing and Characterization of Bituminous Materials, CRC Press, 2009.

[33] C. Branca, G. D'Angelo, C. Crupi, K. Khouzami, S. Rifici, G. Ruello, U. Wanderlingh, Role of the OH and NH vibrational groups in polysaccharide-nanocomposite interactions: A FTIR-ATR study on chitosan and chitosan/clay films, Polymer 99 (2016) 614-622.

[34] I.A. Fadzallah, S.R. Majid, M.A. Careem, A.K. Arof, A study on ionic interactions in chitosan–oxalic acid polymer electrolyte membranes, Journal of Membrane Science 463 (2014) 65-72.

[35] A.L.C. Silva, J.C. Ugucioni, S. Correa, J.D. Ardisson, W.A.A. Macedo, J.P. Silva, A.A.C. Cotta, A.D.B. Brito, Synthesis and

characterization of nanocomposites consisting of polyaniline, chitosan and tin dioxide, Mater Chem Phys 216 (2018) 402-412.

[36] F. Farshi Azhar, A. Olad, A. Mirmohseni, Development of novel hybrid nanocomposites based on natural biodegradable polymer–montmorillonite/polyaniline: preparation and characterization, Polymer Bulletin 71(7) (2014) 1591-1610.

[37] E. Ramya, C. Rajashree, P.L. Nayak, D. Narayana Rao, New hybrid organic polymer montmorillonite/chitosan/polyphenylenediamine composites for nonlinear optical studies, Applied Clay Science 150 (2017) 323-332.

[38] D. Nintu Mandal, S.C., Manjaiah, K.M., Dwivedi, B.S., Lata, Nain, Kumar R. Aggarwal, P., Novel chitosan grafted zinc containing nanoclay polymer biocomposite (CZNCPBC): Controlled release formulation (CRF) of Zn2+, Reactive and Functional Polymers 127 (2018) 55-66.

[39] M. Ignat, P. Samoila, C. Cojocaru, L. Sacarescu, V. Harabagiu, Novel Synthesis Route for Chitosan-Coated Zinc Ferrite Nanoparticles as Potential Sorbents for Wastewater Treatment, Chemical Engineering Communications 203(12) (2016) 1591-1599.

[40] P. Samoila, C. Cojocaru, I. Cretescu, C.D. Stan, V. Nica, L. Sacarescu, V. Harabagiu, Nanosized Spinel Ferrites Synthesized by Sol-Gel Autocombustion for Optimized Removal of Azo Dye from Aqueous Solution, Journal of Nanomaterials 2015 (2015) 1-13.

[41] A. Lesbani, S.O. Ceria Sitompul, R. Mohadi, N. Hidayati, Characterization and Utilization of Calcium Oxide (CaO) Thermally Decomposed from Fish Bones as a Catalyst in the Production of Biodiesel from Waste Cooking Oil, Makara Journal of Technology 20(3) (2016) 121.

[42] M.F. Mubarak, A.H. Ragab, R. Hosny, I.A. Ahmed, H.A. Ahmed, S.M. El-Bahy, A. El Shahawy, Enhanced Performance of Chitosan via a Novel Quaternary Magnetic Nanocomposite Chitosan/Grafted Halloysitenanotubes@ZnγFe3O4 for Uptake of

Cr (III), Fe (III), and Mn (II) from Wastewater, Polymers 13(16) (2021) 2714.

[43] T. Szabó, A. Bakandritsos, V. Tzitzios, S. Papp, L. Korösi, G. Galbács, K. Musabekov, D. Bolatova, D. Petridis, I. Dékány, Magnetic iron oxide/clay composites: effect of the layer silicate support on the microstructure and phase formation of magnetic nanoparticles, Nanotechnology 18(28) (2007) 285602.

[44] C. Deng, Q. Huang, X. Zhu, Q. Hu, W. Su, J. Qian, L. Dong, B. Li, M. Fan, C. Liang, The influence of Mn-doped CeO2 on the activity of CuO/CeO2 in CO oxidation and NO + CO model reaction, Applied Surface Science 389 (2016) 1033-1049.

[45] M.M. Abdellatif, S.M.A. Soliman, N.H. El-Sayed, F.H.H. Abdellatif, Iota-carrageenan based magnetic aerogels as an efficient adsorbent for heavy metals from aqueous solutions, Journal of Porous Materials 27(1) (2019) 277-284.

[46] H. Yao, Z. You, L. Li, X. Shi, S.W. Goh, J. Mills-Beale, D. Wingard, Performance of asphalt binder blended with non-modified and polymer-modified nanoclay, Construction and Building Materials 35 (2012) 159-170.

[47] M. Chen, B. Leng, S. Wu, Y. Sang, Physical, chemical and rheological properties of waste edible vegetable oil rejuvenated asphalt binders, Construction and Building Materials 66 (2014) 286-298.

[48] L. Wang, C. Chang, Rheological evaluation of polymer modified asphalt binders, Journal of Wuhan University of Technology-Mater. Sci. Ed. 30(4) (2015) 695-702.

[49] A.A. Ragab, M.M. Mohammedy, M. El-Shafie, Using waste flexible polyvinyl chloride treated with DOP/calcium hydroxide for enriching the performance of oxidizing bitumen, Journal of Thermal Analysis and Calorimetry 136(3) (2018) 1079-1091.

[50] L.K. Aggarwal, P.C. Thapliyal, S.R. Karade, Anticorrosive properties of the epoxy–cardanol resin based paints, Progress in Organic Coatings 59(1) (2007) 76-80.

_____